Atmos. Chem. Phys. Discuss., 8, 9179–9207, 2008
www.atmos-chem-phys-discuss.net/8/9179/2008/

Atmospheric Chemistry and Physics Discussions

Internally mixed soot, sulfates, and organic matter in aerosol particles from Mexico City

K. Adachi[1,2] **and P. R. Buseck**[1,2]

[1]School of Earth and Space Exploration, Arizona State University, Tempe, AZ, USA
[2]Department of Chemistry and Biochemistry, Arizona State University, Tempe, AZ, USA

Received: 7 April 2008 – Accepted: 14 April 2008 – Published: 22 May 2008

Correspondence to: P. R. Buseck (pbuseck@asu.edu)

Published by Copernicus Publications on behalf of the European Geosciences Union.

Abstract

Soot particles are major aerosol constituents that result from emissions of burning of fossil fuel and biomass. Because they both absorb sunlight and contribute to cloud formation, they are an influence on climate on local, regional, and global scales. It is therefore important to evaluate their optical and hygroscopic properties and those effects on the radiation budget. Those properties commonly change through reaction with other particles or gases, resulting in complex internal mixtures. Using transmission electron microscopy, we measured ~8000 particles (25 samples) with aerodynamic diameters from 0.05 to 0.3 μm that were collected in March 2006 from aircraft over Mexico City (MC) and adjacent areas. More than 50% of the particles consist of internally mixed soot, organic matter, and sulfate. Imaging combined with chemical analysis of individual particles show that many are coated, consist of aggregates, or both. Coatings on soot particles can amplify their light absorption, and coagulation with sulfates changes their hygroscopic properties, resulting in shorter lifetime. Our results suggest that a mixture of materials from multiple sources such as vehicles, power plants, and biomass burning occurs in individual particles, thereby increasing their complexity. Through changes in their optical and hygroscopic properties, internally mixed soot particles have a greater effect on the regional climate than uncoated soot particles. Moreover, soot occurs in more than 60% of all particles in the MC plumes, suggesting its important role in the formation of secondary aerosol particles.

1 Introduction

Aerosol particles have important influences on Earth's radiative and hydrological balance (Ramanathan et al., 2001) and human health (Dockery et al., 1993). Knowledge of their contribution to radiative forcing is inadequate (IPCC, 2007). Our study focuses on internal mixtures of soot (black carbon) particles with organic matter (OM) and sulfate collected during the MILAGRO (Megacity Initiative: Local and Global Research

ACPD
8, 9179–9207, 2008

Observations) campaign in and near Mexico City (MC) and their implications for global climate. Many developing megacities, such as MC, are located in tropical areas. Their importance will increase through growing economic activity and populations. Many details of the aerosol particles emitted from tropical megacities are not well known, although they have important effects on the troposphere and people living in it.

Soot particles are emitted through incomplete combustion of fossil fuel and biomass carbon. They produce a net warming effect in the atmosphere through absorption of sunlight (Chung and Seinfeld, 2002, 2005; Jacobson 2001; Haywood et al., 1997; Myhre et al., 1998; Penner et al., 1998; Bond and Bergstrom, 2006). Internally mixed soot particles are estimated to be the second most significant component of global warming after CO_2 in terms of direct radiative forcing (Jacobson, 2001; Ramanathan and Carmichael, 2008).

Here we focus on particles of soot, OM, and sulfate, with emphasis on internally mixed particles. Climate models assume that aerosol particles are single phases (external mixtures), internal mixtures, or both (Jacobson, 2001; Chung and Seinfeld, 2002, 2005; Bond et al., 2006; Takemura et al., 2005) The externally mixed assumption is unrealistic in many atmospheric situations as many, and perhaps most, aerosol particles are internally mixed (e.g., Murphy et al., 2006; Pósfai et al., 1999). Internal mixtures are a better assumption if appropriate morphological and mixing properties are applied to models, although these parameters are commonly not well known. However, such properties affect their optical and hygroscopic properties. Therefore, a detailed analysis of internally mixed particles is appropriate.

We used transmission electron microscopy to analyze the morphologies, sizes, and compositions of individual aerosol particles. The transmission electron microscope (TEM) is a powerful instrument for determining these properties (Buseck and Pósfai, 1999; Buseck and Schwartz, 2003; Niemi et al., 2006; Johnson et al., 2005; Utsunomiya et al., 2004). Soot is a common constituent of such mixtures, and the TEM can be used to recognize it based on its distinctive morphological features. Absent its destruction by instruments such as the particle soot absorption photometer (PSAP)

(Baumgardner et al., 2007), because of the similarity of its chemical properties with OM, it can be difficult to detect by using other instruments. Moreover, several TEM studies have shown that OM with sulfate coatings on soot particles are widespread (e.g., Chen et al., 2006; Kojima et al., 2005; Pósfai et al., 1999; Li et al., 2003; Okada et al., 2005; Johnson et al., 2005).

Our goal is to characterize the chemical and physical properties of internally mixed soot particles in order to understand their hygroscopic properties, optical properties, and coating processes at the individual-particle scale. Using the samples collected from the MC plumes, we also aim to characterize the particles that were emitted from heavily polluted areas, where contributions of aerosol emissions to the regional and global environments are becoming increasingly important.

2 Materials and methods

2.1 Mexico City atmospheric research projects

The MILAGRO campaign was conducted in Mexico during March 2006 (Molina et al., 2008[1]). The goal was to understand the evolution of trace gases and particles from anthropogenic emissions in and around MC, as an example of a tropical megacity. Detailed meteorological conditions during the campaign are discussed in de Foy et al. (2008) and Fast et al. (2007). The prior MCMA-2003 (Mexico City Metropolitan Area field campaign 2003) also revealed important insights into the meteorology, primary pollutant emissions, ambient secondary pollutant precursor concentrations, photochemical oxidant production, and secondary aerosol particle formation in MC (Molina et al., 2007).

[1]Molina, L. T., Madronich, S., Gaffney J., et al.: An overview of the MILAGRO 2006 Campaign: Mexico City emissions and its transport and transformation, Atmos. Chem. Phys. Discuss., in preparation, 2008.

2.2 Sampling

Samples were collected using 3-stage impactor samplers (MPS-3, California Measurements, Inc.). Units were placed in both the NCAR/NSF C130 and the U.S. Forest Service Twin Otter (Yokelson et al., 2007) aircraft. Both contained isokinetic particle inlets with cutoff diameters of a few μm (Jonsson et al., 1995). The 50% cut-off aerodynamic diameters of the samplers are 2.0, 0.3, and 0.05 μm. In this study, we used the smallest impactor stage (0.05 to 0.3 μm). Sampling times were mostly between 4 and 6 min, although they ranged from 3 to 17 min (Table 1) depending on the particle concentrations.

SEM stubs, each having one TEM grid attached, were placed in each stage of the samplers. Lacy carbon grids were used for TEM sample collections. Such grids, which have "spider net" carbon substrates, are designed to be used for chemical analyses and high-resolution imaging (e.g., Figs. 1 and 2). The substrate causes minimal overlap with samples and yields clear images where the particles extend over holes in the substrates (Pósfai et al., 2003).

We acquired 30 samples from the C130 during 10 research flights and 182 samples from the Twin Otter during 12 research flights. Some samples are primarily from the MC plumes and others from biomass burning. In this study we focus on the samples from the MC urban plumes and adjacent areas near MC (Table 1).

Samples were collected from a wide range of locations and weather conditions. We classified the samples as from either within the MC plume (MC sample, 8 samples) or outside of it (17 samples) using the HYSPLIT back-trajectory model of Draxler and Rolph (2003). Except for #14, all MC samples are from within 80 km of the city center (Table 1).

Most MC samples were collected around 02:00 p.m. local time (Table 1), suggesting that most particles were within eight hours or less from emission. These samples include particles that were emitted during the morning rush hour and transported by local and regional air circulation (Fast et al., 2007). On the other hand, it is likely that

ACPD
8, 9179–9207, 2008

samples from outside MC are older than the MC samples, as most do not have definite sources within 1- to 2-day back-trajectories.

2.3 TEM analysis

We used a Tecnai F20 TEM for imaging and electron energy-loss spectroscopy (EELS) analyses and a CM 200 TEM (both from the FEI Corp.) for energy-dispersive X-ray spectrometer (EDS) analyses. Both TEMs were operated at an accelerating voltage of 200 kV.

The EDS analyses were used to measure compositions of particles ranging from nanometers to micrometers in diameter. By using expanded electron beams that included entire particles (~1 μm), averaged compositions of individual particles were determined. We measured all particles in a certain area of a TEM image (~2000 to 5000 magnification) for the analyses. Each area had between 20 and 60 particles. We chose one or two areas from each of 12 samples and analyzed 379 particles in total (Table 1). Thirty-second collection times were used.

2.4 Soot particles, organic matter (OM), and sulfates

Soot particles from MC typically consist of aggregated carbon spheres ranging in diameter from 20 to 100 nanometers, with median about 44 nm. They contain poorly ordered, curved graphitic layers separated by ~0.36 nm (Fig. 1b) and display a sharp π^* peak in EELS analyses. Soot particles can be recognized by their graphitic structure in TEM images even where they are internally mixed with OM, which is typically amorphous. The structural difference causes contrast in TEM images. However, if the grains are too thick (~1 μm), it can be difficult to identify the soot particles. Therefore, although such thick grains are not common in our samples, some internally mixed soot particles could be underestimated. In MC, soot particles mainly come from vehicles, but some come from biomass burning (Moffet et al., 2007; Jiang et al., 2005).

OM commonly coats the surfaces of soot, sulfates, and mineral dust in our samples

ACPD
8, 9179–9207, 2008

(Figs. 1, 2, and 3). In MC, about half the organic carbon comes from motor vehicles, and from 5 to 26% of organic carbon is from biomass burning (Stone et al., 2008). Except for tar balls, which are spherical (Pósfai et al., 2004; Hand et al., 2005), OM lacks a distinctive morphology. OM particles are less sensitive to the electron beam than sulfates, although they shrink slightly after strong radiation.

Sulfates readily decompose when exposed to an electron beam. Many are coated with OM and, when decomposing, they leave a carbonaceous residue (Figs. 1c,d,f) (Pósfai et al., 2003). We used Ca-coated TEM grids to detect H_2SO_4 and $(NH_4)_2SO_4$ using the same method as Kojima et al. (2006), Yamato and Ono (1989), and Yamato and Tanaka (1994). Most droplets did not react with the Ca coatings, which we interpret as indicating our sulfates were neutralized by ammonium. Such neutralization is consistent with the results of DeCarlo et al. (2007) and Moya et al. (2003). The sulfate comes from regional sources such as petrochemical, power plant, and volcanic emissions (Johnson et al., 2006; de Foy et al., 2007; DeCarlo et al., 2007).

2.5 Particle classification

For purposes of this study, we classified particles into categories based on their morphological features described above: 1) internally mixed soot particles (soot with coatings of OM, sulfates, or both; hereafter, we will refer to mixtures of OM and sulfate as OM-S); 2) soot particles without coatings (externally mixed soot); 3) OM-S without soot; 4) tar balls; and 5) others. Category 1 includes soot particles that were attached to or partly coated by OM-S (soot size>OM-S size), which constitute ~20% of this category, and particles that have both soot and mineral or metal particles with OM-S coatings. If no coatings were recognized in the TEM images, the soot particles were included in category 2. All other particles were classified as category 5 and were mostly mineral dust and metal particles, all of which are crystalline and resist decomposition in the electron beam.

ACPD
8, 9179–9207, 2008

2.6 Particle selection

For particle measurements, we selected a single grid square (125×125 μm) from a TEM grid of each sample, using the same method as Kojima et al. (2004). Between 100 and 300 TEM images were recorded for each sample. All particles with diameters greater than 50 nm in those TEM images, typically between 300 and 600 particles per sample, were sized and categorized. A total of more than 7700 particles from 22 samples were used for size measurements and particle categorization (Table 1). The procedure produces uncertainties of less than 10% relative in the pie chart (Fig. 5).

2.7 Particle size measurements

Averaged particle radii were determined by fitting ellipses to the particle outlines and taking the geometric mean of the semi-minor and semi-major axes. If more than two soot-particle aggregates occur in an internal mixture, only the larger one was measured. The rationale was that these larger soot particles have the greatest effect on the particle optical properties.

Many particles containing OM-S were apparently liquid or at least relatively viscous when collected. In these instances, they spread when on the grid (Figs. 1 and 2). We used lacy-carbon support films to minimize the effect. In some cases, they may have decreased in size because of loss of volatile fractions. Vacuum condition causes ~20% of shrinkage for ammonium sulfate particles (Pósfai et al., 1998). We used the same procedure for all samples, and therefore the comparison among our samples is internally consistent.

3 Results

3.1 Nature of aerosol particles

We found that many MC particles are internally mixed. This observation is consistent with the results from single-particle mass spectrometer measurements (Moffet et al., 2007) and scanning and transmission electron microscopy (Doran et al., 2008; Johnson et al., 2005), all of which were used to analyze MC samples. Images of many MC particles show the intimate mixtures of constituent phases. Typical images and compositions of both internally and externally mixed particles are shown in Figs. 1 and 2, respectively.

EDS measurements show that S occurs in more than 90% of all analyzed particles, and more than 70% of these also contain K. Si occurs in 75% of the particles, although discrete mineral grains were not evident. Small peaks in the EDS spectra showed one or more of V, Cr, Mn, Ni, Zn, Sn, Pb, and Bi in 50% of the particles. Other studies also reported metals in MC aerosol particles (e.g., Moffet et al., 2007; Chow et al., 2002; Johnson et al., 2006; Querol et al., 2008).

In order to explore details of the sorts of particles typical of the MC plume, we obtained EELS analyses across a traverse of one such composite particle (Fig. 3). A plot of S, O, N, and K composition vs. position shows a sulfate decomposition residue (e.g., Point 4 in Fig. 3). The high π^*/σ^* ratios at, e.g., point 1, confirm the identity of soot. The low π^*/σ^* ratios at points 2 and 5 and the lack of a well-defined shape are consistent with the identity of OM.

3.2 Sizes and aspect ratios of aerosol particles

The size distributions of MC samples are similar to those collected outside of MC (Fig. 4). However, the peak of the distribution for internally mixed OM-S coatings from the MC samples is smaller than that from particles collected outside of MC. Where OM-S coats soot, the particle sizes are larger than those without soot.

The aspect ratio (long axis/short axis) is an indicator of compactness. Averaged aspect ratios (and standard deviations) are 2.2 (0.9), 2.1 (0.9), and 1.9 (0.8) for uncoated soot and that with coatings from MC and outside of MC, respectively. Although particles become more compact during aging, those in our samples are not highly compacted but retain their chain-like structure.

3.3 Volumes and number fractions of aerosol particles

The volumes of particles are important for evaluating their optical properties and aging. Most particles have irregular shapes on TEM grids, but many were presumably liquid within the atmosphere. For simplification, we approximated their shapes as roughly elliptical when on the TEM grid. We used their measured semi-major and semi-minor axes to calculate their volumes. The volumes, V, of the soot particles within the internally mixed particles were determined using the relation $V=4/3\times\pi\times a^3\times N$, where a is the radius and N is the number of monomers. N was estimated from the statistical scaling law of fractal aggregates, $N=k_a\times(R_g/a)^{Df}$, where k_a is the structural coefficient, R_g is the radius of gyration, and D_f is the fractal dimension (Adachi et al., 2007). We used the measured semi-major axes of soot particles for determination of R_g (R_g=semi-major axis/1.5) (Brasil et al., 2001; Köylü et al., 1995; Gwaze et al., 2006). For simplification, we divided the soot particles into their extreme values of either open or compact. For soot particles that have aspect ratios >2.0 (open clusters), we used D_f=2.4 and k_a=0.7 (Adachi et al., 2007). For the compacted soot particles (aspect ratios ≤2.0), we used D_f=2.6 and k_a=2.1 (Adachi et al., 2007; Liu and Mishchenko, 2005).

Approximately 80% and 50% by volume of the OM-S particles collected from MC and outside of MC, respectively, contained soot particles. The median value of soot volume fractions for internally mixed particles was 15% when the median monomer radius 22 nm was used and ranged from 10 to 22% for the range of our a (from 10 to 50 nm).

The number fractions of the major particle types also indicate that internally mixed

ACPD
8, 9179–9207, 2008

particles dominated the MC samples (Fig. 5). Soot occurs in 62 and 35% of all particles in the samples from MC and outside MC, respectively, and more than 80% of them were coated by OM-S in both sample sets.

4 Discussion

4.1 OM-S coatings on soot particles

Most MC soot is embedded in or coated by OM-S. The proportion of internally mixed soot is higher than that reported by Okada et al. (2005) for Australia, Hara et al. (2003) for the Arctic, and Hasegawa and Ohta (2002) for Japan and Alaska, even though most of our MC samples were less aged. Since our MC samples were collected close to their sources, generally within less than eight hours after emission and yet were coated when collected, we conclude that the rate of coating was rapid, consistent with the results of Doran et al. (2007), Johnson et al. (2005), and Baumgardner et al. (2007). The rate is much faster than that used in climate models. For example, Cooke et al. (1999) suggested that an exponential lifetime of hydrophobic soot is 1.15 days. Coated soot particles are removed by wet deposition and have shorter lifetimes, which reduces their radiative forcing (van Poppel et al., 2005).

The coated soot particles retained their chain-like structure even though their aspect ratios showed that they were compacted slightly during aging (Abel et al., 2003). A possible explanation is that rapidly deposited coatings covered the entire soot particle and fixed its structure before it became completely compacted.

Light absorption of soot is enhanced when it is coated by OM-S. In our samples, the median coating fraction is 85% by volume in internally mixed particles. Such coatings focus sunlight on the soot and also enlarge the available absorption cross section (Fuller et al., 1999; Chýlek et al., 1995; Bond et al., 2006; Barnard et al., 2007). By using Mie theory, calculations show that a spherical soot core surrounded by a concentric shell has its absorption enhanced by roughly 1.5 relative to one without a coating (Bond

ACPD
8, 9179–9207, 2008

et al., 2006). However, such a configuration probably overestimates the light absorption of our soot particles that are not completely compacted because soot monomers located away from the center of the particle have reduced absorption (Fuller et al., 1999; Bond et al., 2006).

In our MC samples, soot particles occur in 62% of OM-S particles, and 80% by volume of all OM-S particles contain soot. These results suggest that soot particles are important seeds for the development and growth of secondary aerosol particles.

4.2 Contributions from biomass burning

Biomass burning is one of the most important sources of aerosol particles in MC (Moffet et al., 2007; Stone et al., 2008; Yokelson et al., 2007). K is a key element for identifying such particles (Andreae 1983; Li et al., 2003; Pósfai et al., 2003; Hudson et al., 2004; Murphy et al., 2006). In our samples, K occurs in more than 60% of the particles, most of which are sulfates. Sulfate condensation on the biomass-burning particles probably occurred during transport, as was also observed in biomass-burning particles in southern Africa (Pósfai et al., 2003; Gaudichet et al., 1995; Andreae et al., 1998; Gao et al., 2003; Kreidenweis et al., 2001; Liu et al., 2000).

K concentrations are variable among particles (Figs. 1, 2, 3). Some were presumably produced by biomass burning outside of MC. Such burning occurred during the campaign in the central and southern parts of Mexico such as Yucatan and around MC (Yokelson et al., 2007; Fast et al., 2007). Locally, cooking is another source of K-bearing particles (Moffet et al., 2007).

Tar balls are also an indicator of biomass burning (Pósfai et al., 2004). Their number fractions were smaller than those in other areas that had large contributions of biomass burning such as southern Africa, Hungary (Pósfai et al., 2004), and Yosemite National Park (Hand et al., 2005). The relatively low biomass-burning contribution is consistent with the study by Stone et al. (2008).

4.3 Sulfate implications

Sulfate particles are commonly smaller than 200 nm across and are attached to soot, OM, or their mixtures (Fig. 1). Although in areas such as the northern Atlantic Ocean (Pósfai et al., 1999) and southern Finland (Niemi et al., 2006) sulfates encapsulate entire soot particles, the dominant material in the MC samples is OM, and the sulfate as well as soot are either embedded within the OM or attached to its edges. The difference arises because the MC plume included large quantities of OM (Salcedo et al., 2006; Jiang et al., 2005; Zavala et al., 2006; Stone et al., 2008; Querol et al., 2008; Takahama et al., 2007; DeCarlo et al., 2007; Molina et al., 2007; Kleinman et al., 2008), which produced coatings on the soot before the sulfate particles developed. The attached sulfates hardly enhance the light absorption of soot (Mishchenko et al., 2004). On the other hand, the sulfates change the OM and soot particles from hydrophobic to hydrophilic and eventually make them efficient cloud condensation nuclei (CCN) (Lohmann et al., 2004; King et al., 2007). CCN activity influences the formation and properties of clouds, which are important cooling contributors to Earth's radiative balance (Lohmann and Feichter, 2005).

5 Conclusions

Over 50% of the aerosol particles that we sampled from the MC plume consist of internally mixed soot, OM, and sulfates. MC sulfate commonly contains K, suggesting a contribution from biomass burning. These findings suggest that individual particles typically contain materials from multiple sources. OM is a dominant material in the MC plume, and soot particles are common. As a result, OM rapidly coats most soot particles. Additionally, sulfate commonly attaches to OM and soot particles, changing them from hydrophobic to hydrophilic.

In a city where pollution is heavy and formation of secondary organics is rapid, as is the case in MC, assuming that soot particles are internally mixed is relatively reliable for

modeling. Depending on their nature, the coatings can have either negative or positive effects on the radiative forcing. They reduce soot lifetimes in the atmosphere through the changes in particle hygroscopicity and increased mass, which together result in both washout and dry deposition and, on the other hand, they amplify light absorption. Such shorter lifetimes and stronger absorption of coated soot, compared to uncoated ones, suggest that it has significant influences on the radiation budget in the regional area and eventually climate. Since soot is the dominant primary particle in many urban areas, its properties, especially when coated, are important for accurate evaluation of its effects on local and regional climate. Moreover, soot occurs in more than 60% of all particles in the MC plumes, suggesting its important role in the formation of secondary aerosol particles.

Acknowledgements. The authors thank T. Karl, F. Flocke, and S. Madronich for their help with collection of the C130 samples and R. Yokelson, T. Christian, S. Urbanski, C. Wold, D. Toohey, M. Fisher, E. Thompson, G. Moore, J. Stright, A. Knobloch, and K. Bailey for their help with collection of Twin Otter samples. C. Wilson and J. Cagle helped greatly with the aircraft inlets. We are grateful to E. Freney, L. Garvie, and S. H. Chung for their discussions of this manuscript. We gratefully acknowledge the use of TEMs within the LeRoy Eyring Center for Solid State Science at Arizona State University. This study was supported by NSF grant ATM-0531926.

References

Abel, S. J., Haywood, J. M., Highwood, E. J., Li, J., and Buseck, P. R.: Evolution of biomass burning aerosol properties from an agricultural fire in southern Africa, Geophys. Res. Lett., 30, 1783, doi:10.1029/2003GL017342, 2003.

Adachi, K., Chung, S. H., Friedrich, H., and Buseck, P. R.: Fractal parameters of individual soot particles determined using electron tomography: Implications for optical properties, J. Geophys. Res.-Atmos., 112, D14202, doi:10.1029/2006JD8296, 2007.

Andreae, M. O.: Soot carbon and excess fine potassium: long-range transport of combustion-derived aerosols, Science, 220, 1148–1151, 1983.

Andreae, M. O., Andreae, T. W., Annegarn, H., Beer, J., Cachier, H., Le Canut, P., Elbert, W.,

Maenhaut, W., Salma, I., Wienhold, F. G., and Zenker, T.: Airborne studies of aerosol emissions from savanna fires in southern Africa: 2. Aerosol chemical composition, J. Geophys. Res.-Atmos., 103, 32 119–32 128, 1998.

Barnard, J. C., Kassianov, E. I., Ackerman, T. P., Johnson, K., Zuberi, B., Molina, L. T., and Molina, M. J.: Estimation of a "radiatively correct" black carbon specific absorption during the Mexico City Metropolitan Area (MCMA) 2003 field campaign, Atmos. Chem. Phys., 7, 1645–1655, 2007, http://www.atmos-chem-phys.net/7/1645/2007/.

Baumgardner, D., Kok, G. L., and Raga, G. B.: On the diurnal variability of particle properties related to light absorbing carbon in Mexico City, Atmos. Chem. Phys., 7, 2517–2526, 2007, http://www.atmos-chem-phys.net/7/2517/2007/.

Bond, T. C. and Bergstrom, R. W.: Light absorption by carbonaceous particles: An investigative review, Aerosol Sci. Technol., 40, 27–67, 2006.

Bond, T. C., Habib, G., and Bergstrom, R. W.: Limitations in the enhancement of visible light absorption due to mixing state, J. Geophys. Res.-Atmos., 111, D20211, doi:10.1029/2006JD007315, 2006.

Brasil, A. M., Farias, T. L., Carvalho, M. G., and Koylu, U. O.: Numerical characterization of the morphology of aggregated particles, J. Aerosol Sci., 32, 489–508, 2001.

Buseck, P. R. and Pósfai, M.: Airborne minerals and related aerosol particles: Effects on climate and the environment, P. Natl. Acad. Sci. USA., 96, 3372–3379, 1999.

Buseck, P. R. and Schwartz, S. E.: Tropospheric aerosols, in: Treatise on Geochemistry, 4, edited by: Turekian, K. K. and Holland, H.D., Elsevier Science Ltd., San Diego, 91–142, 2003.

Chen, Y. Z., Shah, N., Huggins, F. E., and Huffman, G. P.: Microanalysis of ambient particles from Lexington, KY, by electron microscopy, Atmos. Environ., 40, 651–663, 2006.

Chow, J. C., Watson, J. G., Edgerton, S. A., and Vega, E.: Chemical composition of $PM_{2.5}$ and PM_{10} in Mexico City during winter 1997, Sci. Total Environ., 287, 177–201, 2002.

Chung, S. H. and Seinfeld, J. H.: Global distribution and climate forcing of carbonaceous aerosols, J. Geophys. Res.-Atmos., 107, D19, 4407, doi:10.1029/2001JD001397, 2002.

Chung, S. H. and Seinfeld, J. H.: Climate response of direct radiative forcing of anthropogenic black carbon, J. Geophys. Res.-Atmos., 110, D11102, doi:10.1029/2004JD005441, 2005.

Chýlek, P., Videen, G., Ngo, D., Pinnick, R. G., and Klett, J. D.: Effect of black carbon on the optical properties and climate forcing of sulfate aerosols, J. Geophys. Res.-Atmos., 100, 16 325–16 332, 1995.

Cooke, W. F., Liousse, C., Cachier, H., and Feichter, J.: Construction of a 1 degrees x 1 degrees fossil fuel emission data set for carbonaceous aerosol and implementation and radiative impact in the ECHAM4 model, J. Geophys. Res.-Atmos., 104, 22 137–22 162, 1999.

de Foy, B., Fast, J. D., Paech, S. J., Phillips, D., Walters, J. T., Coulter, R. L., Martin, T. J., Pekour, M. S., Shaw, W. J., Kastendeuch, P. P., Marley, N. A., Retama, A., and Molina, L. T.: Basin-scale wind transport during the MILAGRO field campaign and comparison to climatology using cluster analysis, Atmos. Chem. Phys., 8, 1209–1224, 2008, http://www.atmos-chem-phys.net/8/1209/2008/.

de Foy, B., Lei, W., Zavala, M., Volkamer, R., Samuelsson, J., Mellqvist, J., Galle, B., Martínez, A. P., Grutter, M., Retama, A., and Molina, L. T.: Modelling constraints on the emission inventory and on vertical dispersion for CO and SO_2 in the Mexico City Metropolitan Area using Solar FTIR and zenith sky UV spectroscopy, Atmos. Chem. Phys., 7, 781–801, 2007, http://www.atmos-chem-phys.net/7/781/2007/.

DeCarlo, P. F., Dunlea, E. J., Kimmel, J. R., Aiken, A. C., Sueper, D., Crounse, J., Wennberg, P. O., Emmons, L., Shinozuka, Y., Clarke, A., Zhou, J., Tomlinson, J., Collins, D. R., Knapp, D., Weinheimer, A. J., Montzka, D. D., Campos, T., and Jimenez, J. L.: Fast airborne aerosol size and chemistry measurements with the high resolution aerosol mass spectrometer during the MILAGRO Campaign, Atmos. Chem. Phys. Discuss., 7, 18 269–18 317, 2007.

Dockery, D. W., Pope, C. A., Xu, X. P., Spengler, J. D., Ware, J. H., Fay, M. E., Ferris, B. G., and Speizer, F. E.: An association between air pollution and mortality in 6 United States cities, New Engl. J. Med., 329, 1753–1759, 1993.

Doran, J. C., Barnard, J. C., Arnott, W. P., Cary, R., Coulter, R., Fast, J. D., Kassianov, E. I., Kleinman, L., Laulainen, N. S., Martin, T., Paredes-Miranda, G., Pekour, M. S., Shaw, W. J., Smith, D. F., Springston, S. R., and Yu, X. Y.: The T1-T2 study: evolution of aerosol properties downwind of Mexico City, Atmos. Chem. Phys., 7, 1585–1598, 2007, http://www.atmos-chem-phys.net/7/1585/2007/.

Doran, J. C., Fast, J. D., Barnard, J. C., Laskin, A., Desyaterik, Y., and Gilles, M. K.: Applications of lagrangian dispersion modeling to the analysis of changes in the specific absorption of elemental carbon, Atmos. Chem. Phys., 8, 1377–1389, 2008, http://www.atmos-chem-phys.net/8/1377/2008/.

Draxler, R. R. and Rolph, G. D.: HYSPLIT (HYbrid Single-Particle Lagrangian Integrated Trajectory) Model access via NOAA ARL READY Website (http://www.arl.noaa.gov/ready/hysplit4.html), NOAA Air Resources Laboratory, Silver

Spring, MD, 2003.
Fast, J. D., de Foy, B., Rosas, F. A., Caetano, E., Carmichael, G., Emmons, L., Mckenna, D., Mena, M., Skamarock, W., Tie, X., Coulter, R. L., Barnard, J. C., Wiedinmyer, C., and Madronich, S.: A meteorological overview of the MILAGRO field campaigns, Atmos. Chem. Phys., 7, 2233–2257, 2007, http://www.atmos-chem-phys.net/7/2233/2007/.
Fuller, K. A., Malm, W. C., and Kreidenweis, S. M.: Effects of mixing on extinction by carbonaceous particles, J. Geophys. Res.-Atmos., 104, 15 941–15 954, 1999.
Gao, S., Hegg, D. A., Hobbs, P. V., Kirchstetter, T. W., Magi, B. I., and Sadilek, M.: Water-soluble organic components in aerosols associated with savanna fires in southern Africa: Identification, evolution, and distribution, J. Geophys. Res.-Atmos., 108, D13, 8491, doi:10.1029/2002JD002324, 2003.
Gaudichet, A., Echalar, F., Chatenet, B., Quisefit, J. P., Malingre, G., Cachier, H., Buatmenard, P., Artaxo, P., and Maenhaut, W.: Trace elements in tropical African savanna biomass burning aerosols, J. Atmos. Chem., 22, 19–39, 1995.
Gwaze, P., Schmid, O., Annegarn, H. J., Andreae, M. O., Huth, J., and Helas, G.: Comparison of three methods of fractal analysis applied to soot aggregates from wood combustion, J. Aerosol Sci., 37, 820–838, 2006.
Hand, J. L., Malm, W. C., Laskin, A., Day, D., Lee, T., Wang, C., Carrico, C., Carrillo, J., Cowin, J. P., Collett, J., and Iedema, M. J.: Optical, physical, and chemical properties of tar balls observed during the Yosemite Aerosol Characterization Study, J. Geophys. Res.-Atmos., 110, D21210, doi:10.1029/2004JD005728, 2005.
Hara, K., Yamagata, S., Yamanouchi, T., Sato, K., Herber, A., Iwasaka, Y., Nagatani, M., and Nakata, H.: Mixing states of individual aerosol particles in spring Arctic troposphere during ASTAR 2000 campaign, J. Geophys. Res.-Atmos., 108, D7, 4209, doi:10.1029/2002JD002513, 2003.
Hasegawa, S. and Ohta, S.: Some measurements of the mixing state of soot-containing particles at urban and non-urban sites, Atmos. Environ., 36, 3899–3908, 2002.
Haywood, J. M., Roberts, D. L., Slingo, A., Edwards, J. M., and Shine, K. P.: General circulation model calculations of the direct radiative forcing by anthropogenic sulfate and fossil-fuel soot aerosol, J. Climate, 10, 1562–1577, 1997.
Hudson, P. K., Murphy, D. M., Cziczo, D. J., Thomson, D. S., De Gouw, J. A., Warneke, C., Holloway, J., Jost, J. R., and Hübler, G.: Biomass-burning particle measurements: Characteristic composition and chemical processing, J. Geophys. Res.-Atmos., 109, D23S27,

doi:10.1029/2003JD004398, 2004.
IPCC: Climate Change 2007: The Physical Science Basis. Contribution of Working Group I to the Fourth Assessment Report of the Intergovernmental Panel on Climate Change, edited by: Solomon, S., Qin, D., Manning, M., Chen, Z., Marquis, M., Averyt, K. B., Tignor, M., and Miller, H. L. Cambridge University Press, Cambridge, United Kingdom and New York, NY, USA, 996 pp., 2007.
Jacobson, M. Z.: Strong radiative heating due to the mixing state of black carbon in atmospheric aerosols, Nature, 409, 695–697, 2001.
Jiang, M., Marr, L. C., Dunlea, E. J., Herndon, S. C., Jayne, J. T., Kolb, C. E., Knighton, W. B., Rogers, T. M., Zavala, M., Molina, L. T., and Molina, M. J.: Vehicle fleet emissions of black carbon, polycyclic aromatic hydrocarbons, and other pollutants measured by a mobile laboratory in Mexico City, Atmos. Chem. Phys., 5, 3377–3387, 2005, http://www.atmos-chem-phys.net/5/3377/2005/.
Johnson, K. S., Zuberi, B., Molina, L. T., Molina, M. J., Iedema, M. J., Cowin, J. P., Gaspar, D. J., Wang, C., and Laskin, A.: Processing of soot in an urban environment: case study from the Mexico City Metropolitan Area, Atmos. Chem. Phys., 5, 3033–3043, 2005, http://www.atmos-chem-phys.net/5/3033/2005/.
Johnson, K. S., de Foy, B., Zuberi, B., Molina, L. T., Molina, M. J., Xie, Y., Laskin, A., and Shutthanandan, V.: Aerosol composition and source apportionment in the Mexico City Metropolitan Area with PIXE/PESA/STIM and multivariate analysis, Atmos. Chem. Phys., 6, 4591–4600, 2006, http://www.atmos-chem-phys.net/6/4591/2006/.
Jonsson, H. H., Wilson, J. C., Brock, C. A., Knollenberg, R. G., Newton, R., Dye, J. E., Baumgardner, D., Borrmann, S., Ferry, G. V., Pueschel, R., Woods, D. C., and Pitts, M. C.: Performance of a focused cavity aerosol spectrometer for measurements in the stratosphere of particle size in the 0.06–2.0-μm-diameter range, J. Atmos. Ocean. Tech., 12, 115–129, 1995.
Katrinak, K. A., Rez, P., and Buseck, P. R.: Structural variations in individual carbonaceous particles from an urban aerosol, Environ. Sci. Technol., 26, 1967–1976, 1992.
King, S. M., Rosenoern, T., Shilling, J. E., Chen, Q., and Martin, S. T.: Cloud condensation nucleus activity of secondary organic aerosol particles mixed with sulfate, Geophys. Res. Lett., 34, L24806, doi:10.1029/2007GL030390, 2007.
Kleinman, L. I., Springston, S. R., Daum, P. H., Lee, Y.-N., Nunnermacker, L. J., Senum, G. I., Wang, J., Weinstein-Lloyd, J., Alexander, M. L., Hubbe, J., Ortega, J., Canagaratna, M.

R., and Jayne, J.: The time evolution of aerosol composition over the Mexico City plateau, Atmos. Chem. Phys., 8, 1559–1575, 2008, http://www.atmos-chem-phys.net/8/1559/2008/.
Kojima, T., Buseck, P. R., Wilson, J. C., Reeves, J. M., and Mahoney, M. J.: Aerosol particles from tropical convective systems: Cloud tops and cirrus anvils, J. Geophys. Res.-Atmos., 109, D12201, doi:10.1029/2003JD004504, 2004.
Kojima, T., Buseck, P. R., and Reeves, J. M.: Aerosol particles from tropical convective systems: 2. Cloud bases, J. Geophys. Res.-Atmos., 110, D09203, doi:10.1029/2004JD005173, 2005.
Kojima, T., Buseck, P. R., Iwasaka, Y., Matsuki, A., and Trochkine, D.: Sulfate-coated dust particles in the free troposphere over Japan, Atmos. Res., 82, 698–708, 2006.
Köylü, Ü. Ö., Faeth, G. M., Farias, T. L., and Carvalho, M. G.: Fractal and projected structure properties of soot aggregates, Combust. Flame, 100, 621–633, 1995.
Kreidenweis, S. M., Remer, L. A., Bruintjes, R., and Dubovik, O.: Smoke aerosol from biomass burning in Mexico: Hygroscopic smoke optical model, J. Geophys. Res.-Atmos., 106, 4831–4844, 2001.
Li, J., Pósfai, M., Hobbs, P. V., and Buseck, P. R.: Individual aerosol particles from biomass burning in southern Africa: 2, Compositions and aging of inorganic particles, J. Geophys. Res.-Atmos., 108, D13, 8484, doi:10.1029/2002JD002310, 2003.
Liu, X. D., Van Espen, P., Adams, F., Cafmeyer, J., and Maenhaut, W.: Biomass burning in southern Africa: Individual particle characterization of atmospheric aerosols and savanna fire samples, J. Atmos. Chem., 36, 135–155, 2000.
Liu, L. and Mishchenko, M. I.: Effects of aggregation on scattering and radiative properties of soot aerosols, J. Geophys. Res.-Atmos., 110, D11211, doi:10.1029/2004JD005649, 2005.
Lohmann, U., Broekhuizen, K., Leaitch, R., Shantz, N., and Abbatt, J.: How efficient is cloud droplet formation of organic aerosols?, Geophys. Res. Lett., 31, L05108, doi:10.1029/2003GL018999, 2004.
Lohmann, U. and Feichter, J.: Global indirect aerosol effects: a review, Atmos. Chem. Phys., 5, 715–737, 2005, http://www.atmos-chem-phys.net/5/715/2005/.
Mishchenko, M. I., Liu, L., Travis, L. D., and Lacis, A. A.: Scattering and radiative properties of semi-external versus external mixtures of different aerosol types, J. Quant. Spectrosc. Ra., 88, 139–147, 2004.
Moffet, R. C., de Foy, B., Molina, L. T., Molina, M. J., and Prather, A.: Measurement of ambient aerosols in northern Mexico City by single particle mass spectrometry, Atmos. Chem. Phys. Discuss., 7, 6413–6457, 2007, http://www.atmos-chem-phys-discuss.net/7/6413/2007/.

Molina, L. T., Kolb, C. E., de Foy, B., Lamb, B. K., Brune, W. H., Jimenez, J. L., Ramos-Villegas, R., Sarmiento, J., Paramo-Figueroa, V. H., Cardenas, B., Gutierrez-Avedoy, V., and Molina, M. J.: Air quality in North America's most populous city-overview of the MCMA-2003 campaign, Atmos. Chem. Phys., 7, 2447–2473, 2007, http://www.atmos-chem-phys.net/7/2447/2007/.

Moya, M., Castro, T., Zepeda, M., and Baez, A.: Characterization of size-differentiated inorganic composition of aerosols in Mexico City, Atmos. Environ., 37, 3581–3591, 2003.

Murphy, D. M., Cziczo, D. J., Froyd, K. D., Hudson, P. K., Matthew, B. M., Middlebrook, A. M., Peltier, R. E., Sullivan, A., Thomson, D. S., and Weber, R. J.: Single-particle mass spectrometry of tropospheric aerosol particles, J. Geophys. Res.-Atmos., 111, D23S32, doi:10.1029/2006JD007340, 2006.

Myhre, G., Stordal, F., Restad, K., and Isaksen, I. S. A.: Estimation of the direct radiative forcing due to sulfate and soot aerosols, Tellus B, 50, 463–477, 1998.

Niemi, J. V., Saarikoski, S., Tervahattu, H., MäKelä, T., Hillamo, R., VehkamäKi, H., Sogacheva, L., and Kulmala, M.: Changes in background aerosol composition in Finland during polluted and clean periods studied by TEM/EDX individual particle analysis, Atmos. Chem. Phys., 6, 5049–5066, 2006, http://www.atmos-chem-phys.net/6/5049/2006/.

Okada, K., Ikegami, M., Zaizen, Y., Tsutsumi, Y., Makino, Y., Jensen, J. B., and Gras, J. L.: Soot particles in the free troposphere over Australia, Atmos. Environ., 39, 5079–5089, 2005.

Penner, J. E., Chuang, C. C., and Grant, K.: Climate forcing by carbonaceous and sulfate aerosols, Clim. Dynam., 14, 839–851, 1998.

Pósfai, M., Xu, H. F., Anderson, J. R., and Buseck, P. R.: Wet and dry sizes of atmospheric aerosol particles: An AFM-TEM study, Geophys. Res. Lett., 25, 1907–1910, 1998.

Pósfai, M., Anderson, J. R., Buseck, P. R., and Sievering, H.: Soot and sulfate aerosol particles in the remote marine troposphere, J. Geophys. Res.-Atmos., 104, 21 685–21 693, 1999.

Pósfai, M., Simonics, R., Li, J., Hobbs, P. V., and Buseck, P. R.: Individual aerosol particles from biomass burning in southern Africa: 1. Compositions and size distributions of carbonaceous particles, J. Geophys. Res.-Atmos., 108, D13, 8483, doi:10.1029/2002JD002291, 2003.

Pósfai, M., Gelencsér, A., Simonics, R., Arató, K., Li, J., Hobbs, P. V., and Buseck, P. R.: Atmospheric tar balls: Particles from biomass and biofuel burning, J. Geophys. Res.-Atmos., 109, D06213, doi:10.1029/2003JD004169, 2004.

Querol, X., Pey, J., MinguillóN, M. C., PéRez, N., Alastuey, A., Viana, M., Moreno, T., Bernabé, R. M., Blanco, S., Cárdenas, B., Vega, E., Sosa, G., Escalona, S., Ruiz, H., and ArtíñAno, B.:

PM speciation and sources in Mexico during the MILAGRO-2006 Campaign, Atmos. Chem. Phys., 8, 111–128, 2008, http://www.atmos-chem-phys.net/8/111/2008/.
Ramanathan, V., Crutzen, P. J., Kiehl, J. T., and Rosenfeld, D.: Atmosphere-Aerosols, climate, and the hydrological cycle, Science, 294, 2119–2124, 2001.
Ramanathan, V. and Carmichael, G.: Global and regional climate changes due to black carbon, Nature Geosci., 1, 221–227, 2008.
Salcedo, D., Onasch, T. B., Dzepina, K., Canagaratna, M. R., Zhang, Q., Huffman, J. A., DeCarlo, P. F., Jayne, J. T., Mortimer, P., Worsnop, D. R., Kolb, C. E., Johnson, K. S., Zuberi, B., Marr, L. C., Volkamer, R., Molina, L. T., Molina, M. J., Cardenas, B., Bernabé, R. M., Márquez, C., Gaffney, J. S., Marley, N. A., Laskin, A., Shutthanandan, V., Xie, Y., Brune, W., Lesher, R., Shirley, T., and Jimenez, J. L.: Characterization of ambient aerosols in Mexico City during the MCMA-2003 campaign with Aerosol Mass Spectrometry: results from the CENICA Supersite, Atmos. Chem. Phys., 6, 925–946, 2006, http://www.atmos-chem-phys.net/6/925/2006/.
Stone, E. A., Snyder, D. C., Sheesley, R. J., Sullivan, A. P., Weber, R. J., and Schauer, J. J.: Source apportionment of fine organic aerosol in Mexico City during the MILAGRO experiment 2006, Atmos. Chem. Phys., 8, 1249–1259, 2008, http://www.atmos-chem-phys.net/8/1249/2008/.
Takahama, S., Gilardoni, S., Russell, L. M., and Kilcoyne, A. L. D.: Classification of multiple types of organic carbon composition in atmospheric particles by scanning transmission X-ray microscopy analysis, Atmos. Environ., 41, 9435–9451, 2007.
Takemura, T., Nozawa, T., Emori, S., Nakajima, T. Y., and Nakajima, T.: Simulation of climate response to aerosol direct and indirect effects with aerosol transport-radiation model, J. Geophys. Res.-Atmos., 110, D02202, doi:10.1029/2004JD005029, 2005.
Utsunomiya, S., Jensen, K. A., Keeler, G. J., and Ewing, R. C.: Direct identification of trace metals in fine and ultrafine particles in the Detroit urban atmosphere, Environ. Sci. Technol., 38, 2289–2297, 2004.
van Poppel, L. H., Friedrich, H., Spinsby, J., Chung, S. H., Seinfeld, J. H., and Buseck, P. R.: Electron tomography of nanoparticle clusters: Implications for atmospheric lifetimes and radiative forcing of soot, Geophys. Res. Lett., 32, L24811, doi:10.1029/2005GL024461, 2005.
Yamato, M. and Ono, A.: Chemical and physical properties of stratospheric aerosol particles in the vicinity of tropopause folding, J. Meteorol. Soc. Jpn., 67, 147–166, 1989.
Yamato, M. and Tanaka, H.: Aircraft observations of aerosols in the free marine troposphere

over the North Pacific Ocean: Particle chemistry in relation to air mass origin, J. Geophys. Res., 99, D3, 5353–5378, 1994.

Yokelson, R. J., Urbanski, S. P., Atlas, E. L., Toohey, D. W., Alvarado, E. C., Crounse, J. D., Wennberg, P. O., Fisher, M. E., Wold, C. E., Campos, T. L., Adachi, K., Buseck, P. R., and Hao, W. M.: Emissions from forest fires near Mexico City, Atmos. Chem. Phys., 7, 5569–5584, 2007, http://www.atmos-chem-phys.net/7/5569/2007/.

Zavala, M., Herndon, S. C., Slott, R. S., Dunlea, E. J., Marr, L. C., Shorter, J. H., Zahniser, M., Knighton, W. B., Rogers, T. M., Kolb, C. E., Molina, L. T., and Molina, M. J.: Characterization of on-road vehicle emissions in the Mexico City Metropolitan Area using a mobile laboratory in chase and fleet average measurement modes during the MCMA-2003 field campaign, Atmos. Chem. Phys., 6, 5129–5142, 2006, http://www.atmos-chem-phys.net/6/5129/2006/.

Table 1. Samples analyzed in this study.

Sample#	Aircraft	Latitude	Longitude	Altitude (Km)	Distance from MC[a] (Km)	Start time (Local Time)	Sampling time (second)	Sampling date (2006/)	Location[b]	Analyses[c]
1	C130	18.00	260.82	3.2	166	12:27:00	266	03/08	outside	S
2	C130	18.81	260.79	3.0	79	14:33:52	257	03/08	MC	S
3	C130	19.23	260.97	4.1	30	15:17:26	277	03/08	MC	S&E
4	C130	21.00	262.27	2.4	216	10:35:25	267	03/10	outside	S
5	C130	19.71	260.86	3.7	28	14:44:45	332	03/10	MC	S&E
6	C130	21.30	261.87	3.0	220	13:34:12	995	03/12	outside	S
7	C130	20.41	261.84	3.5	136	17:30:01	242	03/12	outside	S
8	C130	21.50	258.34	2.8	367	11:29:16	284	03/16	outside	S&E
9	C130	22.20	259.75	4.1	327	10:50:02	346	03/18	outside	S
10	C130	22.20	259.90	3.5	321	12:32:43	250	03/18	outside	S
11	C130	20.00	260.97	3.8	55	14:54:37	255	03/18	MC	S&E
12	C130	24.97	265.34	4.8	768	14:44:34	248	03/19	outside	S&E
13	C130	24.25	263.57	3.2	594	17:13:37	246	03/19	outside	S&E
14	C130	21.90	262.01	4.0	286	18:29:34	247	03/19	MC	S&E
15	C130	20.08	263.53	4.2	286	11:38:48	251	03/22	outside	S
16	C130	19.73	260.73	4.1	40	14:48:55	250	03/22	MC	S
17	C130	18.53	264.01	4.8	348	16:30:04	356	03/23	outside	S
18	C130	20.64	261.84	4.1	155	5:33:08	309	03/28	outside	S
19	C130	19.85	264.67	4.9	405	6:30:07	310	03/28	outside	S
20	C130	20.01	261.60	3.7	86	11:32:23	348	03/29	outside	S&E
21	C130	20.00	261.11	3.5	57	12:55:29	256	03/29	outside	S&E
22	C130	19.50	260.71	3.7	32	13:38:52	249	03/29	MC	S
23	TO	19.32	260.82	4.1	28	15:43:33	180	03/17	MC	E
24	TO	19.06	263.55	1.5	284	16:58:00	300	03/28	outside	E
25	TO	19.17	267.82	3.7	751	16:31:00	420	03/29	outside	E

[a] 19.5° N and 99° W are used for the center of MC.
[b] Outside indicates samples collected from outside of the MC plume. MC indicates samples collected from the MC plume.
[c] S indicates samples used for size measurements (Fig. 4) and number fraction analysis (Fig. 5), and E indicates samples used for EDS analysis. Samples marked S&E were used for both types of analyses. TO=Twin Otter.

ACPD
8, 9179–9207, 2008

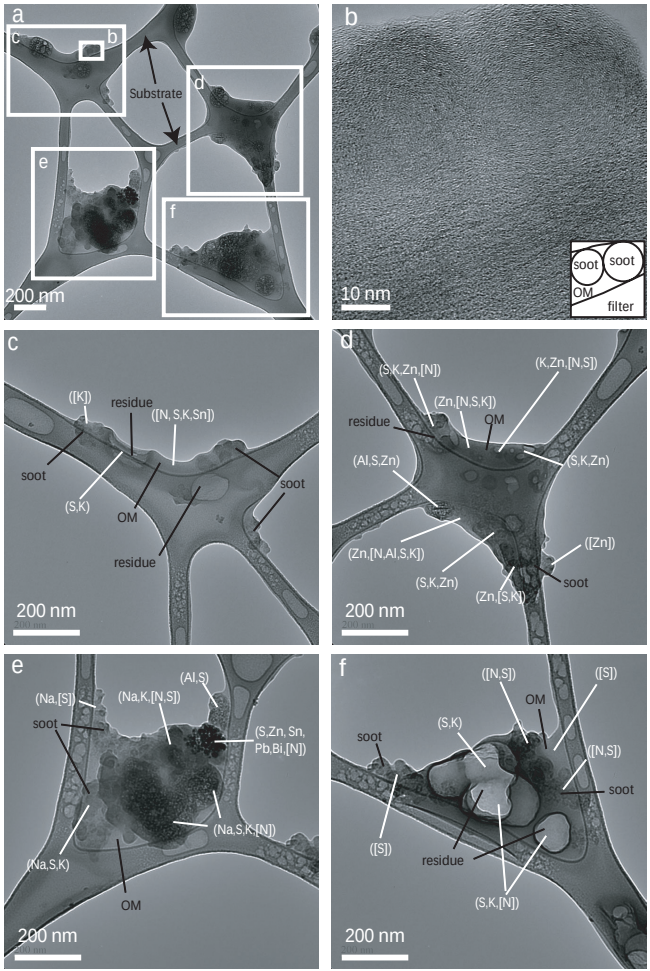

Fig. 1.

ACPD
8, 9179–9207, 2008

Fig. 1. Morphologies and compositions of internally mixed particles. Particles were deposited on lacy carbon filters. This sample was collected from MC (Sample #3 in Table 1). EDS analyses typically indicate minor to trace amounts of the elements in the other phases. **(a)** Low-magnification image of particles c to f. **(b)** High-resolution image of soot particles, OM, and filter. The lower-right illustration shows a sketch of the image. Soot particles have curved graphitic layers. OM and the filter, both of which consist of amorphous carbon, have disordered structures. **(c–f)** Typical images of internally mixed particles; their compositions were obtained using EDS and are given in parentheses, with the results shown in white. Elements in square brackets are in concentrations <1 wt%. C, O, and Si occur in all particles and are not shown in the figure. Soot, OM, and residue, which are indicated using black lines, were identified from their morphological properties.

ACPD
8, 9179–9207, 2008

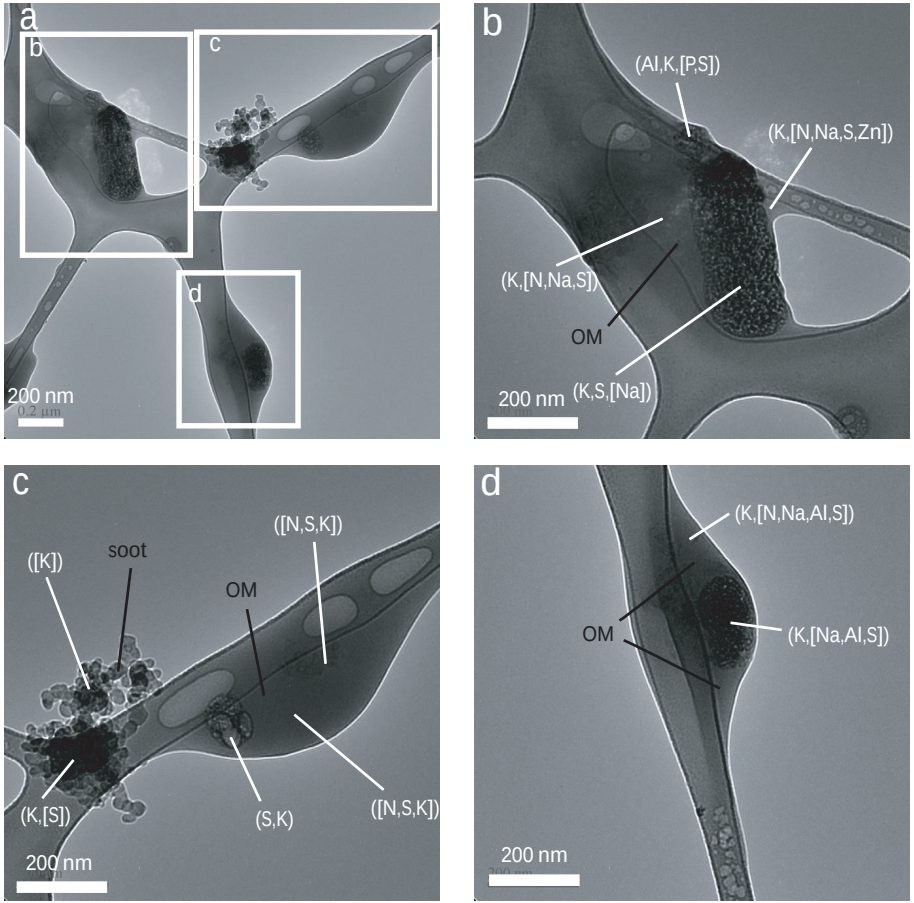

Fig. 2. Morphologies and compositions of externally mixed OM-S and soot particles. Experimental conditions are the same as those in Fig. 1.

ACPD
8, 9179–9207, 2008

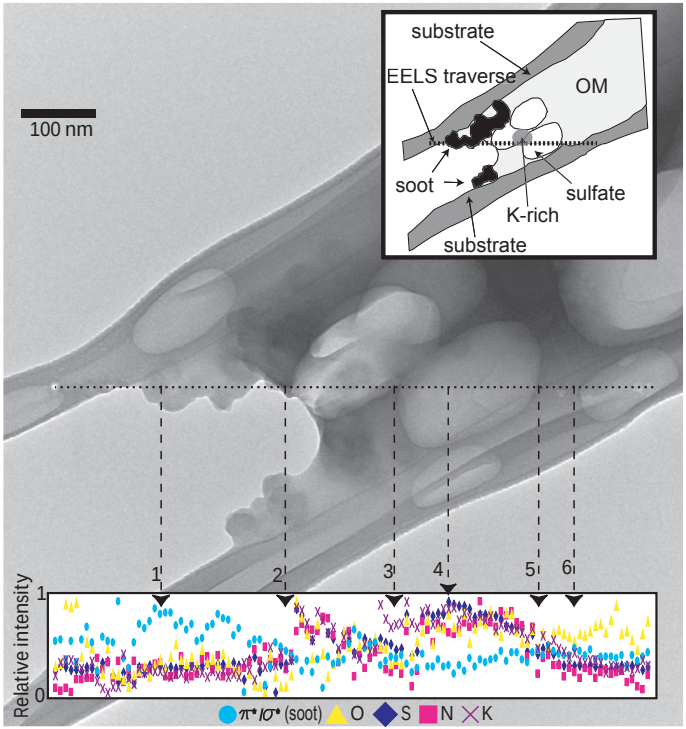

Fig. 3. Plot of composition vs. position in the internally mixed particle from the MC pollution plume (Sample #3). The sketch in the upper right shows the various species. Points 1-soot, 2-OM, 3-K-rich particle, 4-sulfate decomposition residue, 5-OM, 6-lacy-carbon filter. A total of 114 points were analyzed by using EELS at 10 nm intervals. The π^* and σ^* intensities were obtained by using the same method as Katrinak et al. (1992). We used intensities at 184.5, 294.5/σ^*, and 402.5 eV in the EELS spectra for determining the relative abundances of S, K, and N, respectively. For O, total counts ranging from 531.5 to 536.5 eV were used. Exponential background extractions were applied.

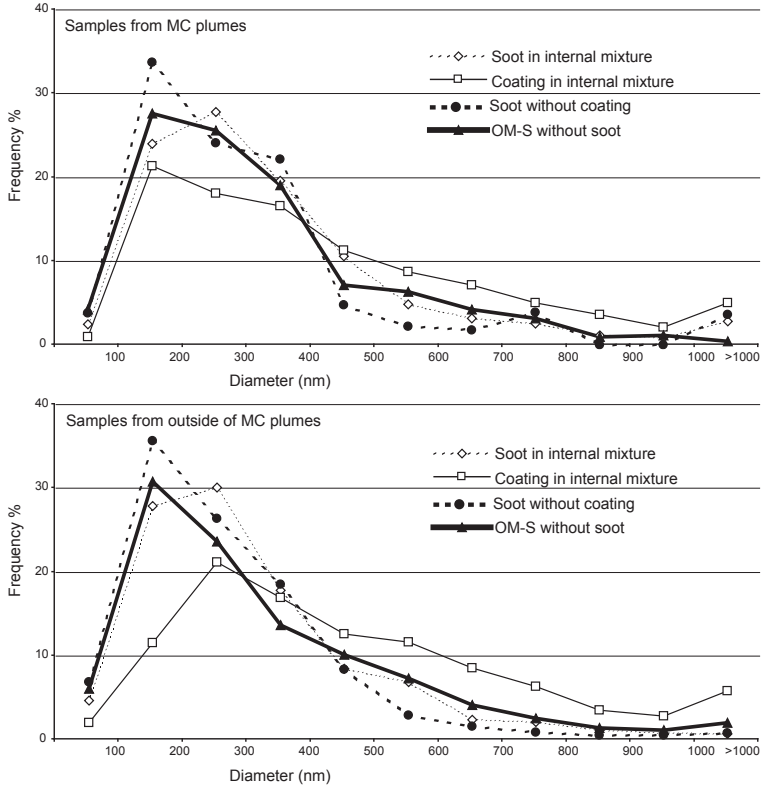

Fig. 4. Distributions of particle diameters. Total numbers of internally mixed particles, soot without coatings, and OM-S without soot are 1312, 176, and 789, respectively, and those of the samples from outside MC are 1492, 378, and 2989, respectively.

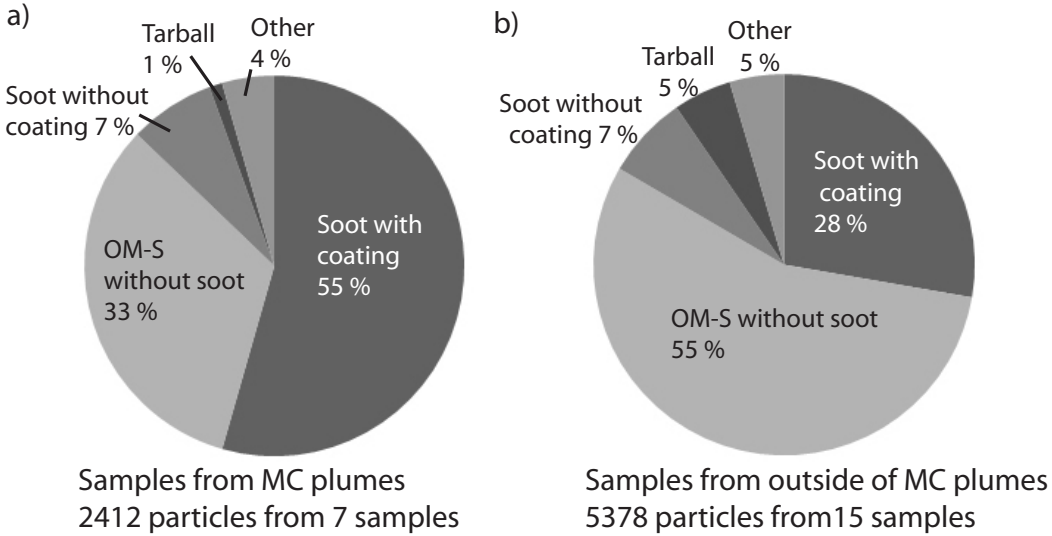

Fig. 5. Number fraction of particles.

ACPD
8, 9179–9207, 2008